Molecular Biology of the Cell
Vol. 10, 179–195, January 1999

Urokinase-Type Plasminogen Activator Receptor Is Internalized by Different Mechanisms in Polarized and Nonpolarized Madin–Darby Canine Kidney Epithelial Cells

Frederik Vilhardt,*† Morten Nielsen,‡ Kirsten Sandvig,§ and Bo van Deurs*

*Structural Cell Biology Unit, Department of Medical Anatomy, The Panum Institute, University of Copenhagen, DK-2200 Copenhagen, Denmark; ‡Department of Medical Biochemistry, University of Århus, DK-8000 Århus, Denmark; and §Institute for Cancer Research, The Norwegian Radium Hospital, 0310 Oslo, Norway

Submitted July 21, 1998; Accepted September 10, 1998
Monitoring Editor: Suzanne R. Pfeffer

Accumulated data indicate that endocytosis of the glycosylphosphatidyl-inositol-anchored protein urokinase plasminogen activator receptor (uPAR) depends on binding of the ligand uPA:plasminogen activator inhibitor-1 (PAI-1) and subsequent interaction with internalization receptors of the low-density lipoprotein receptor family, which are internalized through clathrin-coated pits. This interaction is inhibited by receptor-associated protein (RAP). We show that uPAR with bound uPA:PAI-1 is capable of entering cells in a clathrin-independent process. First, HeLa^{K44A} cells expressing mutant dynamin efficiently internalized uPA:PAI-1 under conditions in which transferrin endocytosis was blocked. Second, in polarized Madin–Darby canine kidney (MDCK) cells, which expressed human uPAR apically, the low basal rate of uPAR ligand endocytosis, which could not be inhibited by RAP, was increased by forskolin or phorbol ester (phorbol 12-myristate 13-acetate), which selectively up-regulate clathrin-independent endocytosis from the apical domain of epithelial cells. Third, in subconfluent nonpolarized MDCK cells, endocytosis of uPA:PAI-1 was only decreased marginally by RAP. At the ultrastructural level uPAR was largely excluded from clathrin-coated pits in these cells and localized in invaginated caveolae only in the presence of cross-linking antibodies. Interestingly, a larger fraction of uPAR in nonpolarized relative to polarized MDCK cells was insoluble in Triton X-100 at 0°C, and by surface labeling with biotin we also show that internalized uPAR was mainly detergent insoluble, suggesting a correlation between association with detergent-resistant membrane microdomains and higher degree of clathrin-independent endocytosis. Furthermore, by cryoimmunogold labeling we show that 5–10% of internalized uPAR in nonpolarized, but not polarized, MDCK cells is targeted to lysosomes by a mechanism that is regulated by ligand occupancy.

INTRODUCTION

The urokinase plasminogen activator receptor (uPAR)[1] is a 55- to 60-kDa glycoprotein (Roldan *et al*., 1990) anchored in the membrane by a glycosylphosphatidyl-inositol (GPI) moiety (Ploug *et al*., 1991). uPAR binds pro-urokinase plasminogen activator (pro-uPA), active two-chain uPA, and uPA complexed with plasminogen activator inhibitor-1 (PAI-1) with high affinity (K_d, ~1 nM). Although first recognized for its role in regulation of plasmin-mediated pericellular proteolysis (Danø *et al*., 1994), uPAR has recently been identified as a cellular adhesion receptor for vitronectin (Wei *et al*., 1994) and as a chemokinesis-

† Corresponding author. E-mail address: f.vilhardt@mai.ku.dk.

[1] Abbreviations used: DFP, diisopropyl fluorophosphate; DMEM, Dulbecco's modified Eagles's medium; DSS, disuccinimidyl suberate; GPI, glycosylphosphatidyl-inositol; LDLR, low-density lipoprotein receptor; LRP, low-density lipoprotein receptor–related protein; MDCK, Madin–Darby canine kidney; MPR, mannose 6-phosphate receptor; PAI, plasminogen activator inhibitor; PBS-CM, PBS with calcium and magnesium; RAP, receptor-associated protein; TCA, trichloroacetic acid; TX-100, Triton X-100; uPA, urokinase plasminogen activator; uPAR, urokinase plasminogen activator receptor.

inducing signaling receptor (Busso *et al.*, 1994; Fazioli *et al.*, 1997). In the cell types examined so far, uPAR associated with uPA is endocytosed slowly like other GPI-anchored proteins (Cubellis *et al.*, 1990; Estreicher *et al.*, 1990; Lemansky *et al.*, 1990; Lisanti *et al.*, 1990; Keller *et al.*, 1992). Being attached to the outer lipid leaflet of the membrane, these proteins lack cytoplasmic internalization signals, and the endocytic route(s) taken by GPI-anchored proteins remains poorly understood. However, when receptor-bound uPA reacts with PAI-1 to form a covalent uPA:PAI-1 complex, a rapid internalization of the complex takes place (Cubellis *et al.*, 1990; Olson *et al.*, 1992). This process is mediated by interaction of uPA:PAI-1 with members of the low-density lipoprotein receptor (LDLR) family, including low-density lipoprotein receptor–related protein (LRP), very–low-density lipoprotein receptor, and most likely also megalin (Herz *et al.*, 1992; Nykjær *et al.*, 1992; Conese *et al.*, 1995; Heegaard *et al.*, 1995), which confer endocytosis through clathrin-coated pits by virtue of tyrosine-based internalization motifs in their cytoplasmic tails. As shown for LRP (Olson *et al.*, 1992; Conese *et al.*, 1995; Nykjær *et al.*, 1997), but likely also applying for megalin and very–low-density lipoprotein receptor (Andreasen *et al.*, 1994; Heegaard *et al.*, 1995), internalization of the uPA:PAI-1 complex occurs concurrently with endocytosis of uPAR itself. Endocytosis of uPA:PAI-1 can be blocked by exogenous addition of receptor-associated protein (RAP) (Li *et al.*, 1994; Conese *et al.*, 1995; Heegaard *et al.*, 1995), a 40-kDa intracellular protein that functions as a chaperone for LRP in the biosynthetic pathway (Bu *et al.*, 1995; Willnow *et al.*, 1996) and blocks binding of all established ligands, including uPA:PAI-1, to LDLR family members (Nykjær *et al.*, 1992; Moestrup *et al.*, 1993; Heegaard *et al.*, 1995).

However, RAP is not able to completely inhibit uPA:PAI-1 internalization, and also, uPA is endocytosed at a low basal level (Cubellis *et al.*, 1990; Estreicher *et al.*, 1990; Conese *et al.*, 1994). The nature of this RAP noninhibitable endocytosis of uPAR is unknown, but the cation-independent mannose 6-phosphate receptor (MPR), which was recently shown to bind uPAR (Nykjær *et al.*, 1998), may contribute to internalization through clathrin-coated pits. Also, uPAR has been associated with detergent-insoluble, glycolipid-rich membrane microdomains (Schnitzer *et al.*, 1995; Wei *et al.*, 1996) and in the presence of cross-linking antibodies with caveolae (Stahl and Mueller, 1995), which have both been suggested to participate in endocytosis of GPI-anchored proteins (Simons and Ikonen, 1997). At least a fraction of internalized uPAR and other GPI-linked proteins are recycled to the cell surface (van den Bosch *et al.*, 1988; Keller *et al.*, 1992; Rijnboutt *et al.*, 1996; Nykjær *et al.*, 1997), although some studies have indicated that a major proportion is retained intracellularly (Rijnboutt *et al.*, 1996). It is not known whether the itinerary of uPAR follows that of cointernalized LDLR family members.

Because uPAR internalization, with a few exceptions (Kjøller *et al.*, 1995; Limongi *et al.*, 1995), has mainly been studied in mesenchymal cells, circulating blood cells, and undifferentiated epithelial cell types (Conese and Blasi, 1995), we decided to investigate uPAR internalization and postendocytic sorting in Madin–Darby canine kidney (MDCK) cells stably transfected with human uPAR cDNA. It is known that human uPAR is expressed apically in polarized MDCK cells (Limongi *et al.*, 1995), whereas caveolae (Vogel *et al.*, 1998) and MPR (Prydz *et al.*, 1990) are basolaterally expressed and separated from uPAR by tight junctions. For this reason we characterized uPAR internalization in both polarized MDCK cells and in subconfluent MDCK cells, which by several criteria had not established full polarity, and therefore provided an opportunity for interactions between uPAR and putative endocytosis mediators or other membrane components confined exclusively to the basolateral cell surface in polarized MDCK cells.

MATERIALS and METHODS

Cell Culture and Transfection

MDCK II cells were maintained in Dulbecco's modified Eagle's medium (DMEM) supplemented with 5% FCS, 2 mM glutamine, and antibiotics. uPAR cDNA (a kind gift from Dr. F. Blasi, University of Milan, Milan, Italy) was inserted into the *Eco*RI site of the expression plasmid pTEJ8 (Johansen *et al.*, 1990) where transcription is under the control of the ubiquitin promoter. MDCK II cells were stably transfected with plasmid containing uPAR cDNA or plasmid alone by the calcium phosphate technique, and clones were selected for neomycin tolerance in 650 μg/ml G418 (Life Technologies, Grand Island, NY) and then subcloned once. HeLa^{K44A} cells (kindly donated by Dr. S.L. Schmid, The Scripps Research Institute, La Jolla, CA) were maintained in DMEM containing 10% FCS, 2 mM glutamine, 400 μg/ml G418, 1 μg/ml tetracycline, and antibiotics.

Reagents and Proteins

Two-chain uPA (Trombolysin; Nordic Health Care, Copenhagen, Denmark) was inactivated with diisopropyl fluorophosphate (DFP; Sigma, St. Louis, MO) as described (Nykjær *et al.*, 1990), except that excess DFP was removed by dialyzation. Human PAI-1 was recombinantly expressed in *Escherichia coli* and purified by gel filtration (G25; Pharmacia Biotech, Uppsala, Sweden) and subsequent chromatography on ion-exchange (Mono Q-Sepharose) and heparin-Sepharose columns (Pharmacia Biotech). For complex formation, an excess of PAI-1 was added to two-chain uPA (trombolysin or ukidan; Serono, Aubonne, Switzerland), and uPA:PAI-1 complexes were purified by sequential affinity chromatography on anti-uPA and anti-PAI-1 rabbit polyclonal antibody–conjugated CNBr-Sepharose columns. Recombinant RAP was expressed and purified as described previously (Nykjær *et al.*, 1992). Briefly, the plasmid containing the RAP cDNA fused to a hexahistidine sequence was expressed in *E. coli* BL21DE3 cells and purified on an Ni^{2+} nitriloacetic column. After a second purification on a Q-Sepharose column (Pharmacia Biotech), the purity of RAP was confirmed by SDS-PAGE and staining with Coomassie Brilliant Blue.

Cell Extraction and Chemical Cross-Linking

Polarized or nonpolarized MDCK cells were washed twice in ice-cold PBS with calcium and magnesium (PBS-CM) and extracted on ice in 1% Triton X-100 (TX-100), 150 mM NaCl, 5 mM EDTA, 25 mM Tris-HCl (pH 7.4) (or 2-[*N*-morpholino]ethanesulfonic acid, pH 6.5) containing 1 mM PMSF, 25 μg/ml leupeptin, and 50 μg/ml pepstatin (Sigma). Extraction volume relative to total cell protein was kept constant, and extracts from each dish were homogenized by pipetting and split in two for a further 10-min incubation on ice or at 37°C, respectively, and subsequently centrifuged for 60,000 $\times$ *g* at 4°C. Equal volumes of supernatant were analyzed by nonreducing SDS-PAGE and Western blotting, using affinity-purified rabbit anti-uPAR antibodies (a gift from Dr. A. Nykjær, University of Århus) followed by HRP-conjugated donkey anti-rabbit antibodies. Signal was detected by enhanced chemiluminiscence (Amersham, Arlington Heights, IL), and densiometric quantitation was performed with a Metamorph imaging system (Universal Imaging, West Chester, PA). Alternatively, cells were preincubated with 1 nM [^{125}I]DFP-uPA at 4°C before cross-linking with 1 mM disuccinimidyl suberate (DSS; Pierce, Rockford, IL) in PBS-CM for 60 min at 4°C. The reaction was quenched by a 15-min incubation with 25 mM Tris-HCl (pH 8.1) before extraction in TX-100 as described above.

Iodination of Ligands

Five to 10 μg of two-chain uPA (trombolysin), DFP-uPA, ricin (Sigma), or holo-transferrin (Sigma) were iodinated by the iodogen method. Specific activities ranged from 20 to 50 $\times$ 10^6 cpm/μg of protein. ^{125}I-Labeled uPA:PAI-1 complexes were produced by incubating 5 μg of iodinated two-chain uPA with a 10$\times$ molar excess of PAI-1 (Molecular Innovations, Royal Oak, MI) for 90 min at room temperature. Complex formation was always verified by SDS-PAGE and autoradiography; almost all radioactivity was associated with a band of 95 kDa.

Radioligand Assays

Polarized or nonpolarized MDCK cells, cultured in 6 or 12 wells, were washed twice in HEPES-buffered DMEM supplemented with 2 mM glutamine and 0.2% BSA (DMEM-BSA) and then incubated with [^{125}I]DFP-uPA or [^{125}I]uPA:PAI-1 at a concentration of 500 pM, with or without 100 nM RAP, for 90 min at 4°C. Cells were washed three times on ice with DMEM-BSA and then incubated at 37°C, with or without 100 nM RAP as appropriate. At the times indicated, medium was removed, and trichloroacetic acid (TCA)–soluble and -insoluble counts determined by precipitation with ice-cold 20% TCA containing 3 mg/ml BSA (final concentrations) for 5–10 min on ice. Cell surface-associated ligand was dissociated with ice-cold 100 mM NaCl, 50 mM glycine-HCl (pH 2.8) for 5 min before lysing cells in 1 M NaOH at room temperature. All fractions were then counted in an LKB-Wallac (Gaithersburg, MD) gamma counter. Nonspecific binding was assessed in the presence of 200 nM uPA and was typically between 4 and 15%. When internalization of RAP was measured, cells were preincubated with 1 nM [^{125}I]RAP in the cold and then chased at 37°C for 7 min. After washing, surface-associated and intracellular ligand was recovered in the supernatant and pellet, respectively, after incubation with 0.25% pronase (Sigma) in PBS-CM for 1 h at 4°C. When recycling of uPAR ligands was examined, cells grown in 24 wells were allowed to internalize prebound [^{125}I]DFP-uPA or [^{125}I]uPA:PAI-1 for 10 min at 37°C, in the presence of 0–100 nM RAP as specified, and then acid washed twice for 2 min each on ice to remove ligand remaining on the surface. Control experiments showed that acid treatment stripped 95–98% of surface-bound ligand. Subsequently cells were washed once in DMEM-BSA and returned to 37°C in DMEM-BSA supplemented with 0–100 nM RAP for a further 40 min. To prevent reinternalization of recycled radioligand, 100 nM unlabeled uPA was included in the chase medium. Subsequently, distribution of ligand in medium, acid wash, and alkalic lysate was determined as described above. Nonspecific binding was determined in the presence of 200 nM unlabeled ligand and values corrected accordingly.

Radioligand Uptake in the HeLa^{K44A} Mutant Dynamin-expressing Cell Line

HeLa^{K44A} cells containing a dominant negative mutant of dynamin under the control of a tetracycline-responsive element (Damke *et al.*, 1994) were cultured for 3 d before experiments with (wild-type dynamin expression) or without (mutant dynamin expression) 1 μg/ml tetracyclin. Cells were incubated in DMEM-BSA for 15 min at 37°C, and then iodinated ligands (~150 ng/ml holo-transferrin, 200 ng/ml ricin, or 3 nM uPA:PAI-1) were added, and incubation continued for a further 5 min. Cell surface–associated and intracellular counts were then determined as described above, except that surface-bound ricin was removed by incubation in 0.1 M lactose at 4°C for 1 h. Nonspecific binding was determined in the presence of a 100–200 M excess of cold ligand, and values were corrected accordingly.

Cell Surface Labeling with Biotin

Nonpolarized MDCK cells were incubated twice for 10 min each in PBS-CM on ice and then surface biotinylated twice for 20 min each with 0.5 mg/ml NHS-SS-biotin (Sigma) in PBS-CM at 4°C. After a 10-min incubation in ice-cold DMEM-BSA, cells were then chased in DMEM-BSA at 37°C for the indicated times. Subsequently, cells were washed twice in ice-cold PBS-CM with 10% FCS and then treated with 50 mM mercaptoethane sulfonic acid (Sigma), 100 mM NaCl, 2.5 mM $CaCl_2$, 50 mM Tris-HCl (pH 8.7) three times for 20 min each on ice to remove biotin remaining on the cell surface. After a final 10-min incubation in 5 mg/ml iodoacetamide in PBS-CM with 1% BSA, cells were extracted in TX-100 (pH 7.4) as described above. Clarified extracts were then precleared with protein A-Sepharose beads (Sigma) and immunoprecipitated with affinity-purified anti-uPAR rabbit antibodies overnight at 4°C. Beads were washed twice in extraction buffer and then boiled in SDS sample buffer before separation by 10% SDS-PAGE and transfer to nitrocellulose membranes. After extensive blocking in 3% BSA, 0.1% Tween 20 in PBS, membranes were incubated with HRP-conjugated streptavidin (Amersham) before thorough washing and signal development by ECL.

Immunofluorescence

Nonpolarized MDCK cells cultured overnight in two- or eight-chamber slides (Nunc, Roskilde, Denmark), or filter-grown (Costar Transwells, Cambridge, MA), polarized MDCK cells were incubated for 18 h in normal growth medium containing 100 μg/ml leupeptin and 67 μg/ml pepstatin and either 100 nM DFP-uPA or 100 nM uPA:PAI-1. Cells were then fixed in 2% formaldehyde in phosphate buffer (pH 7.2) overnight at 4°C, washed thoroughly, and nonspecific binding blocked by 5% normal goat serum in PBS containing 0.1% TX-100 or 0.2% saponin for permeabilization. Cells were incubated with the monoclonal anti-uPAR antibody R2 (kindly provided by Dr. E.Rønne, The Finsen Institute, Copenhagen, Denmark; Rønne *et al.*, 1991) for 45 min, washed twice for 5 min each in PBS, and then incubated with Texas Red–conjugated goat anti-mouse antibodies (Southern Biotechnology, Birmingham, AL) for 30 min before wash and a secondary immunolabeling step with rabbit polyclonal antibodies raised against LAMP-1 (a kind gift from Dr. S. Carlsson, University of Umeå, Umeå, Sweden) followed by FITC-conjugated goat anti-rabbit antibodies. Finally slides were rinsed briefly in distilled water and mounted in Fluoromount G (Southern Biotechnology) containing 2.5 mg/ml *N*-propyl-galleate (Sigma). Controls included omission of primary antibodies or the use of irrelevant antibodies and produced only low levels of staining. Slides were examined with a Zeiss LSM 510 confocal laser scanning microscope using a C-Apochromat 63$\times$, 1.2 water immersion objec-

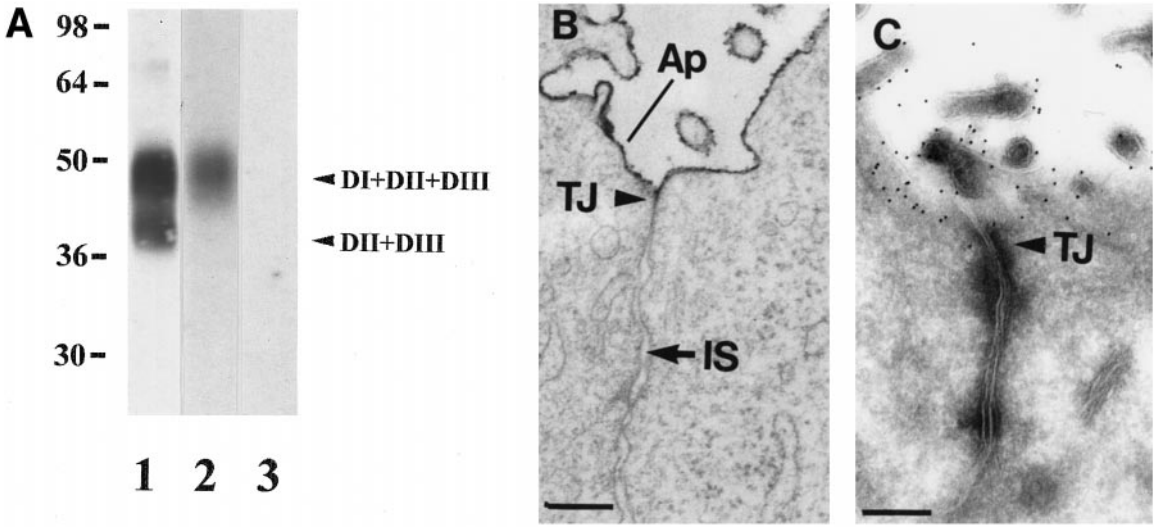

Figure 1. Transfected uPAR is expressed correctly as an apically sorted, GPI-anchored protein and specifically binds DFP-uPA. (A) TX-100 (1%) extracts from transfected MDCK cells were resolved by 10% SDS-PAGE and transferred to nitrocellulose membranes for Western blotting with polyclonal rabbit antibodies that recognize full-length (DI+DII+DIII) and cleaved (DII+DIII) uPAR (lane 1) or ligand blotting with 10 pM [^{125}I]-DFP-uPA alone (lane 2) or 100 nM unlabeled ligand (lane 3). (B) MDCK cells grown to confluency for 4 d in plastic dishes were fixed in the presence of ruthenium red before embedding. Ruthenium red is restricted to the apical (Ap) cell surface and microvilli and excluded from the intercellular space (IS) by tight junctions (TJ). (C) Polarized MDCK cells cultured as in B were fixed and processed for cryoimmunogold labeling with uPAR antibodies followed by 10 nm colloidal gold–conjugated protein A. Labeling is confined to the apical domain by tight junctions (TJ). Bars, 100 nm.

tive (Carl Zeiss, Thornwood, NY), and the 543-nm line of the helium-neon laser or the 488-nm line of the argon laser for excitation of Texas Red and FITC, respectively. Each fluorophore was scanned independently and saved as a 1024 × 1024-pixel image at 8-bit resolution before merging of channels and import into Adobe Photoshop (Adobe Systems, Mountain View, CA) for compilation and direct printing.

Cryoimmunogold Electron Microscopy and Preembedding Labeling

To analyze the distribution of uPAR after a single round of endocytosis, polarized or subconfluent MDCK cells were preincubated for 1–2 h in DMEM-BSA with leupeptin and pepstatin before saturation of uPAR with 10 nM DFP-uPA or uPA:PAI-1 (produced from PAI-1 recombinantly expressed in yeast, kindly donated by Dr. P. Andreasen, University of Århus) at 4°C. Cells were washed once and then incubated in DMEM-BSA with lysosomal inhibitors for 150 min, an interval that was inferred from fluorescence experiments to correspond to near total cell surface clearance of uPA:PAI. Alternatively, nonpolarized MDCK cells were incubated with cationized 20-nm gold for 5 h and chased for 2 h in DMEM-BSA alone and then for a further 3 h in DMEM-BSA containing 10 μg/ml cycloheximide (Sigma) and 50 nM DFP-uPA or uPA:PAI-1. Cells were then washed and fixed in 2% formaldehyde/0.1% glutaraldehyde in 0.2 M HEPES (pH 7.4) at 4°C overnight. Cell samples were embedded in 10% gelatin and infiltrated sequentially with 2.1 and 2.3 M sucrose before freezing in liquid nitrogen. Cryosections (~80 nm) were cut at −110°C with a Reichert Ultracut cryoultramicrotome (Leica, Glostrup, Denmark) and transferred to Formvar carbon-coated copper grids with 2.3 M sucrose or 2% methylcellulose:2.3 M sucrose (1:1). Single or double immunolabeling was performed essentially as described (Slot *et al*., 1991) with polyclonal antibodies to uPAR, MPR-300 (a kind gift from Dr. K. von Figura, University of Göttingen, Göttingen, Germany), and LAMP-1 followed by 10 or 15 nm of colloidal gold-conjugated protein A (purchased from Dr. G. Posthuma, Department of Cell Biology, Medical School, Utrecht University, Utrecht, The Netherlands) as appropriate. Finally grids were contrasted in methylcellulose containing 0.3% uranyl acetate and examined in a JEOL (Tokyo, Japan) 100CX or Philips (Eindhoven, The Netherlands) CM100 electron microscope. For preembedding labeling, nonpolarized MDCK cells were incubated in DMEM-BSA with 1.5 μg/ml anti-uPAR polyclonal antibodies for 60 min at 4°C, followed by washing and incubation with 10 nm of gold-conjugated goat anti-rabbit antibodies (10 μg/ml) for a further 60 min. After final washing, cells were fixed in 2% formaldehyde/0.1% glutaraldehyde in 0.1 M phosphate buffer (pH 7.2) and Epon embedded using standard techniques.

RESULTS

uPAR Expression in Polarized and Nonpolarized MDCK cells

MDCK II cells were stably transfected with human uPAR cDNA, and a clone (clone 3.2) with moderate expression of uPAR was selected for most experiments (unless otherwise indicated). By Western blotting with affinity-purified rabbit antibodies, uPAR was visible as two bands (Figure 1A) corresponding to full-length uPAR and a faster-migrating, cleaved form of uPAR lacking the N-terminal ligand-binding domain. Cleavage, which is promoted by several proteases, including uPA itself, has been observed in neoplastic tissue as well as in cultured cell types (Solberg *et al*., 1994; Høyer-Hansen *et al*., 1997) and also in MDCK cells (Limongi *et al*., 1995). In agreement with

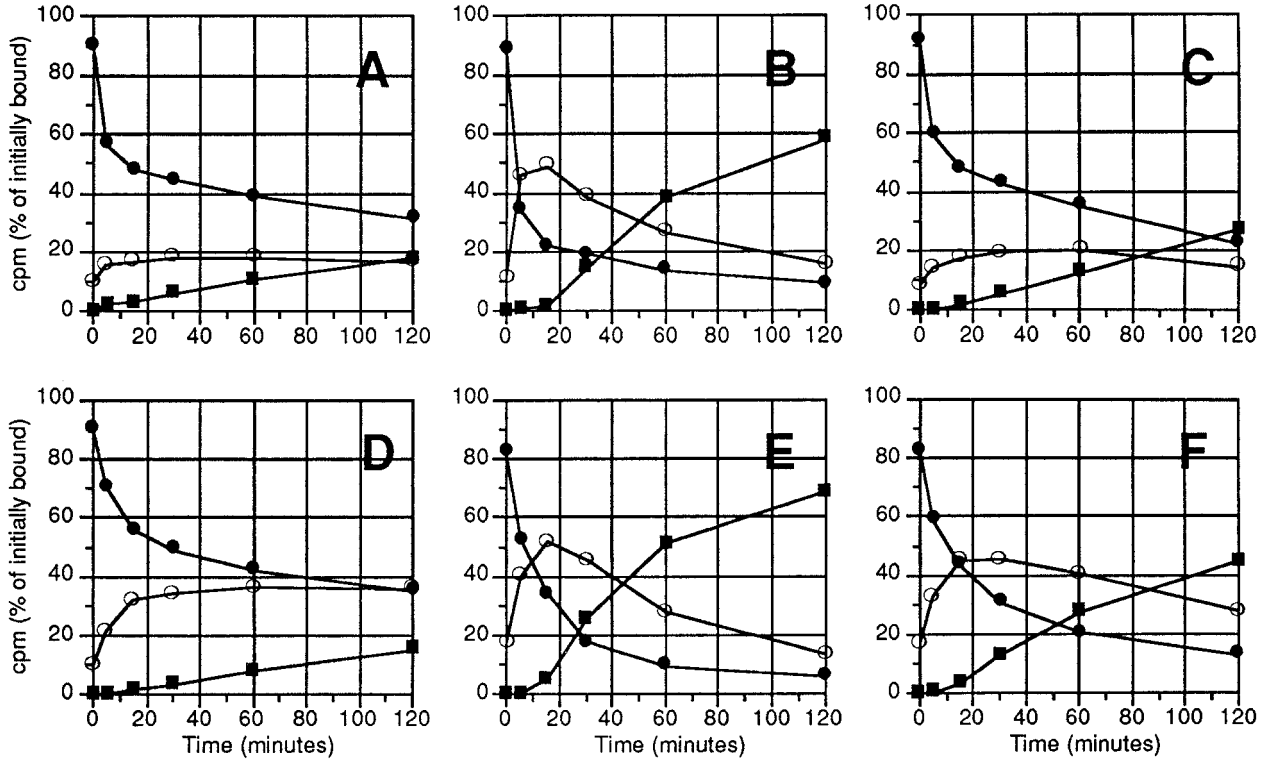

Figure 2. Time course of internalization and degradation of DFP-uPA and uPA:PAI-1 in polarized and nonpolarized MDCK cells. Polarized monolayers cultured for 4 d (A–C) or nonpolarized MDCK cells cultured for 14–16 h (D–F) were incubated with 500 pM [^{125}I]DFP-uPA (A and D) or [^{125}I]uPA:PAI-1 without (B and E) or with (C and F) 100 nM RAP for 90 min at 4°C, washed, and then shifted to 37°C in the absence (B and E) or presence (C and F) of 100 nM RAP. At the times indicated the fraction of ligand present on the cell surface (closed circles) and in the cell lysate (open circles) or as degraded ligand in the medium (squares) was determined as described in MATERIALS AND METHODS and expressed as percentage of total cell-associated counts before shift to 37°C. A representative experiment of three to six independent ones is shown.

this, [^{125}I]DFP-uPA ligand blotting showed only specific binding to full-length uPAR (Figure 1A, lanes 2 and 3). Additionally, uPAR was almost totally releasable with phosphatidylinositol-specific phospholipase C at 37°C, indicating that uPAR was correctly anchored in the membrane by a GPI moiety.

MDCK cells grown to confluency on plastic culture ware formed polarized monolayers with apical microvilli and tight junctions that totally excluded the dye ruthenium red from the intercellular space (Figure 1B). Under these conditions uPAR was exclusively expressed at the apical domain of the cells (Figure 1C) as expected, because GPI anchoring confers apical sorting of proteins in most epithelial cell types (Lisanti *et al.*, 1990; Lisanti and Rodriquez-Boulan, 1990; Simons and Ikonen, 1997). When MDCK cells were seeded at low density and cultured overnight, they were aggregated but well spread. At the ultrastructural level tight junctions were sparse, and most cell surfaces were accessible to ruthenium red; furthermore, uPAR localized with transferrin receptors, MPR, and caveolae (see below) on the dorsal and lateral surfaces of the cells, indicating that full polarity had not been established. For simplicity these cells will henceforth be referred to as nonpolarized MDCK cells.

Polarized and Nonpolarized MDCK Cells Internalize uPAR Ligands by Different Mechanisms

When we analyzed endocytosis of iodinated uPAR ligands from the apical domain of polarized MDCK cells (Figure 2, A–C), our results agreed well with data derived for fibroblastic and monocytic cell lines (Cubellis *et al.*, 1990; Olson *et al.*, 1992; Conese and Blasi, 1995). Thus the fraction of internalized DFP-uPA reached a low steady-state level of ~20%, whereas uPA:PAI-1 was rapidly cleared from the cell surface and degraded. This rapid uptake was completely blocked by the presence of 100 nM RAP in the medium, and under these conditions uPA:PAI-1 internalization was almost identical to that of DFP-uPA (Figure 2, compare A and C).

When endocytosis was examined in nonpolarized MDCK cells, marked differences to apical uptake were evident. At steady state, approximately twice as much

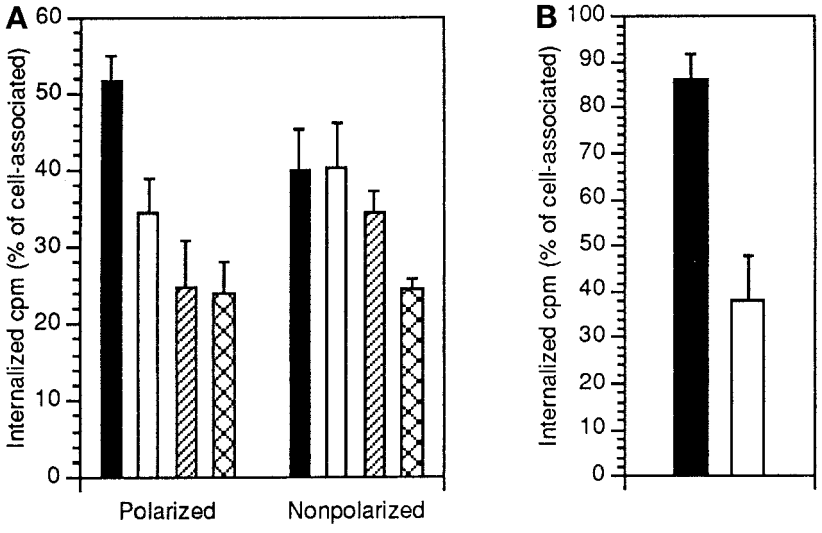

Figure 3. Polarized and nonpolarized MDCK cells show differential sensitivity to inhibition of [^{125}I]uPA:PAI-1 internalization by RAP and excess unlabeled uPA:PAI-1. (A) Polarized or nonpolarized MDCK cells were incubated with 500 pM [^{125}I]uPA:PAI-1 for 90 min at 4°C. After washing cells were incubated for 10 min at 37°C in the absence (black bars) or presence of either a 200-fold molar excess of unlabeled ligand (white bars) or 100 nM RAP (hatched bars). For comparison, endocytosis of prebound [^{125}I]ricin (200 ng/ml) was also determined (cross-hatched bars). Surface-associated and internalized counts were then determined, and results are expressed as internalization index (internalized counts per minute/total cell-associated counts per minute). (B) Polarized (black columns) or nonpolarized (white columns) MDCK cells were incubated with 1 nM [^{125}I]RAP at 4°C and then chased for 7 min at 37°C before measurement of surface-associated and internalized ligand. Results are expressed as internalization index. In both A and B, mean and SD of three independent experiments in duplicate are shown.

DFP-uPA was present intracellularly, and strikingly, 100 nM RAP caused only a minor decrease in uPA:PAI-1 internalization. No further decrease was seen when higher concentrations of RAP were used. Importantly, also in nonpolarized cells both DFP-uPA and uPA:PAI-1 were specifically ligated to uPAR and did not bind alternative basolateral receptors to any appreciable extent, as radioligand binding to mock-transfected cells was negligible. We also tested whether a 200 M excess of unlabeled ligand would interfere with uptake of prebound [^{125}I]uPA:PAI-1 (Figure 3A). In polarized cells this decreased uPA:PAI-1 internalization almost to the same extent as RAP, but again uptake was unaffected in nonpolarized cells. Notably, uPA:PAI-1 endocytosis was higher than ricin uptake, indicating that uPA:PAI-1 internalization did not just represent turnover of bulk membrane (Figure 3A). Although uPA:PAI-1 was endocytosed with comparable efficiency in polarized and nonpolarized cells, internalization efficiency of RAP was decreased in nonpolarized MDCK cells (Figure 3B).

uPAR Can Be Internalized by a Clathrin-independent Mechanism in MDCK and HeLa^{K44A} Cells

GPI-anchored proteins have been reported to be excluded from coated pits (Bretscher *et al.*, 1980) and have been associated with caveolae and uncoated invaginations of the plasma membrane in nonepithelial cell types (Rothberg *et al.*, 1990; Stahl and Mueller, 1995; Keller and Simons, 1998), suggesting clathrin-independent mechanisms of endocytosis. When the surface distribution of uPAR in polarized MDCK cells challenged with uPA:PAI-1 was analyzed by postfixation immunogold labeling, clathrin-coated pits containing uPAR could be readily observed (Figure 4, A–C), in agreement with the observation that apical internalization of uPA:PAI-1 is RAP inhibitable and therefore most likely mediated by members of the LDLR family, which localize in coated pits (Kerjaschki and Farquhar, 1983; Chen *et al.*, 1990; Moestrup *et al.*, 1990; Bu *et al.*, 1994). More importantly, however, we found that in nonpolarized MDCK cells, uPAR with or without bound uPA:PAI-1 was largely excluded from clathrin-coated pits. Even in MDCK clone 8.1 cells (Figure 4, D–F) with very strong expression of uPAR (eight times more than clone 3.2 used for all other experiments), only 0.8% of the total surface labeling for unoccupied uPAR was present in coated pits (Table 1). In nonpolarized MDCK cells incubated with uPA:PAI-1 (Figure 4, G–J) 1.1% of uPAR surface labeling could be found in coated pits. Because we estimated that ~1.3% of the surface area of nonpolarized MDCK cells was occupied by coated pits, it is concluded that uPAR with or without bound uPA:PAI-1 was largely excluded, or at least not concentrated, in coated pits. Additionally, localization in caveolae was very rarely observed but could readily be induced by prefixation cross-linking with antibodies (Figure 4, J and K), as also reported by others (Mayor *et al.*, 1994).

Attempts to block the clathrin-coated pit pathway by cytosol acidification with 10 mM acetic acid (Sandvig *et al.*, 1987) had no effect on uPA:PA-1 internalization in polarized or nonpolarized MDCK cells, likely because acidity in itself may cause immobilization of GPI-anchored proteins (Hannan *et al.*, 1993). Consistent with this, a higher proportion of uPAR was present in the detergent-insoluble fraction when TX-100 extraction was performed at slightly acidic pH (see below), as established for other GPI-anchored proteins (Sargiacomo *et al.*, 1993; Gorodinsky and Harris, 1995). To establish whether uPAR is capable of

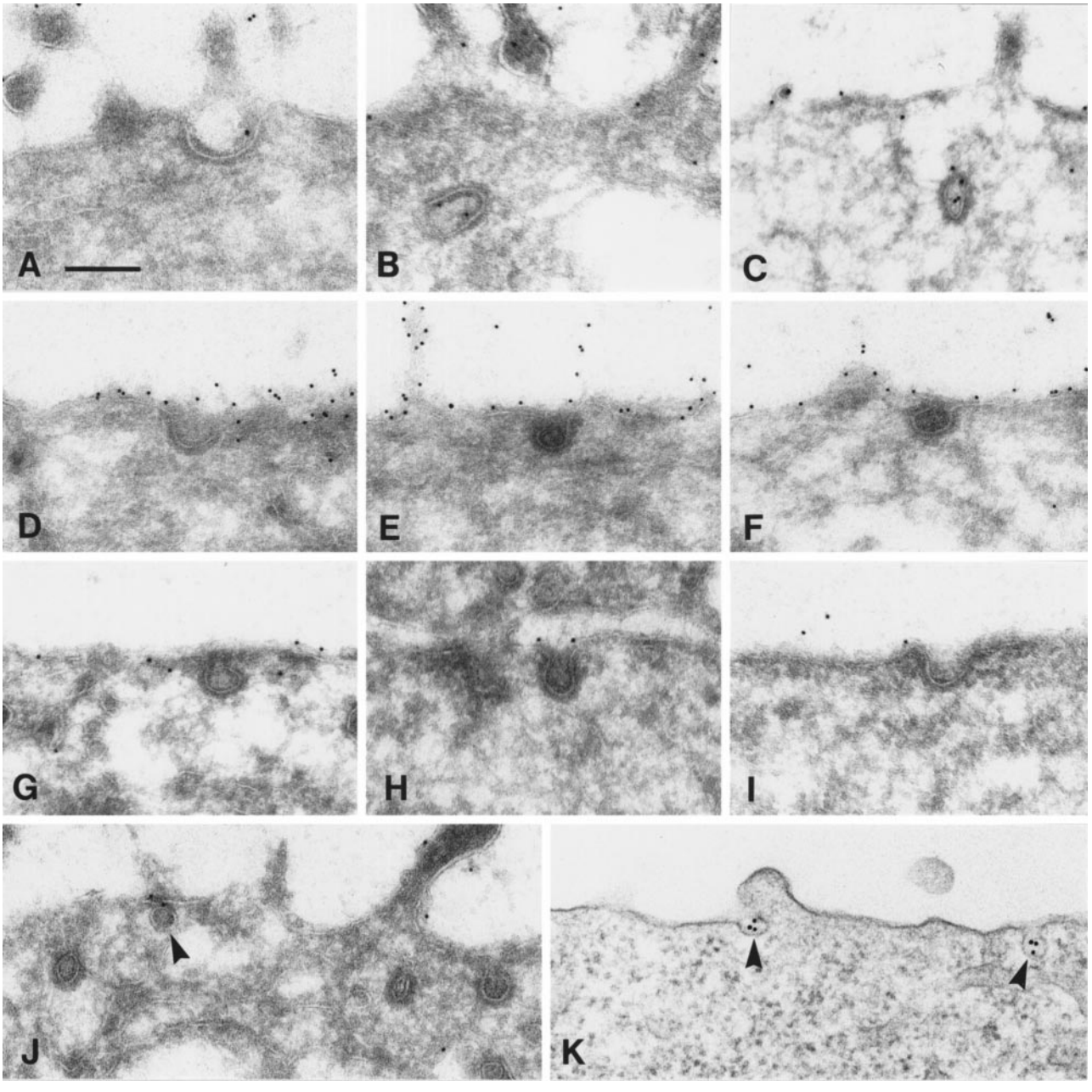

Figure 4. In nonpolarized cells uPAR is excluded from clathrin-coated pits and localizes in caveolae only in the presence of cross-linking antibodies. (A–C) Polarized MDCK cells were incubated with 10 nM uPA:PAI-1 at 4°C and then chased for 10 min at 37°C. Subsequently, cryosections were labeled with anti-uPAR rabbit antibodies followed by protein A-gold (10 nm). Representative images of coated pits containing uPAR are shown. (D–F) Cryosections derived from an MDCK clone (clone 8.1) expressing uPAR at very high levels. Cells were fixed at subconfluency (in the absence of ligand) and labeled for uPAR. (G–J) Nonpolarized MDCK cells (clone 3.2) were challenged with uPA:PAI-1, and cryosections were labeled for uPAR. Note that in both types of experiment (D–J), uPAR was largely excluded from coated pits. Moreover, uPAR in general was also excluded from caveolar profiles (J, arrowhead). (K) Epon section of nonpolarized MDCK cells, which were incubated with anti-uPAR rabbit antibodies (1.5 μg/ml) followed by 10 nm of gold-conjugated goat anti-rabbit antibodies before fixation and processing for electron microscopy. Note clustering of uPAR in caveolae (arrowheads). Bar, 200 nm.

entering cells through a clathrin-independent pathway, we therefore used the HeLa^{K44A} cell line, which carries a dominant negative mutant of dynamin under the control of a tetracycline-responsive system (Damke *et al.*, 1994). When K44A-dynamin is expressed, budding of clathrin-coated vesicles from the

Table 1. Concentration of uPAR in clathrin-coated pits of nonpolarized MDCK cells as determined by immunogold labeling of ultracryosections

	Total no. of gold particles counted	% Gold particles in coated pits	Total amount (length) of surface included (μm)	% of surface occupied by coated pits[a]	Concentration of uPAR in coated pits (fold)
Clone 8.1 (without bound uPA:PAI-1)	8529	0.8	705	~1.3	0.6
Clone 3.2 (with bound uPA:PAI-1)	1095	1.1	730	~1.3	0.8

[a] Calculation of the fractional surface area occupied by coated pits is based on an average of both clones.

plasma membrane is inhibited. As determined by immunofluorescence, HeLa^{K44A} cells express transferrin receptors at a high level and uPAR at moderate levels, and control cells expressing wild-type dynamin preferentially internalize [^{125}I]uPA:PAI-1 relative to [^{125}I]DFP-uPA (our unpublished results). When ligand uptake was examined in K44A-dynamin–expressing cells, transferrin endocytosis, which occurs mainly through clathrin-coated pits, was reduced to 12% normalized to control cells. In contrast, internalization of ricin, serving as a general membrane marker, or uPA:PAI-1 was only slightly decreased (Figure 5).

We next took advantage of the fact that clathrin-independent endocytosis from the apical domain of polarized MDCK cells is up-regulated by activators of adenylate cyclase and protein kinase C (Eker *et al.*, 1994; Holm *et al.*, 1995). Figure 6 shows that forskolin or phorbol 12-myristate 13-acetate selectively increased LDLR family member–independent internalization of uPAR because endocytosis of DFP-uPA, or uPA:PAI-1 in the presence of RAP, was increased, whereas uPA:PAI-1 alone was internalized to the same extent as in untreated control cells.

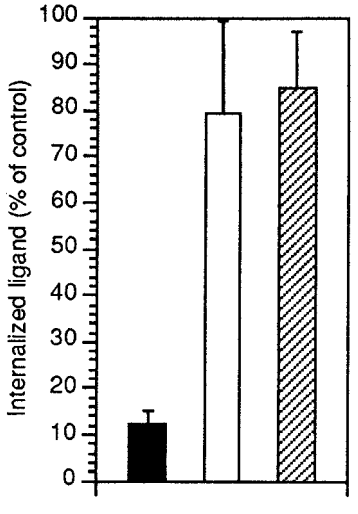

Figure 5. HeLa^{K44A} cells internalize uPA:PAI-1 through a clathrin-independent pathway. HeLa^{K44A} cells were incubated for 5 min at 37°C in the presence of iodinated holo-transferrin (black bars), ricin (white bars), or uPA:PAI-1 (hatched bars) and surface-associated and internal counts per minute were subsequently determined as described in MATERIALS AND METHODS. Results are expressed as internalization index (internalized counts per minute/total cell-associated counts per minute) and normalized relative to control HeLa cells expressing wild-type dynamin. Mean and SD of three independent experiments in duplicate are shown.

Internalized uPAR Is Detergent Insoluble in Nonpolarized MDCK Cells

The mechanism of internalization of GPI-anchored proteins is still poorly characterized but may be re-

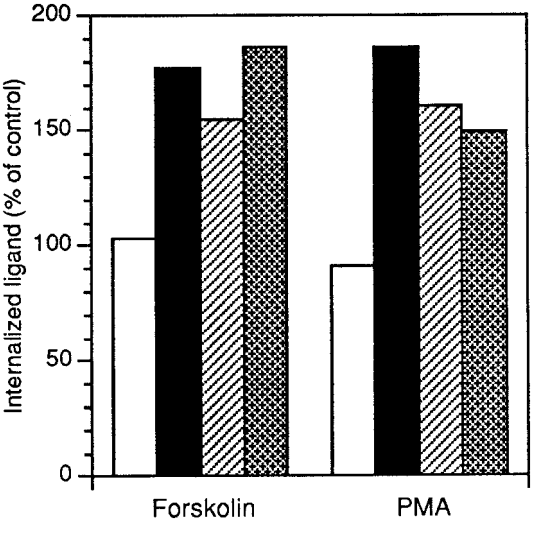

Figure 6. Clathrin-independent uPAR-internalization from the apical domain of polarized MDCK cells is selectively up-regulated by activators of adenylate cyclase or protein kinase C. Filter-grown MDCK cells were preincubated with 100 μM forskolin for 30 min or 250 nM phorbol 12-myristate 13-acetate (PMA) for 15 min before addition of radiolabeled ligands to the apical compartment; 4 nM uPA:PAI-1 without (white columns) or with 100 nm cold RAP (hatched columns), 4 nM DFP-uPA (black columns), or 200 ng/ml ricin (cross-hatched columns). Incubation was continued for a further 8 min at 37°C, and then surface-associated and internal counts were determined as outlined in MATERIALS AND METHODS. The results are expressed as internalization in percentage of uptake in control cells. The means of two experiments with variation <15% are shown.

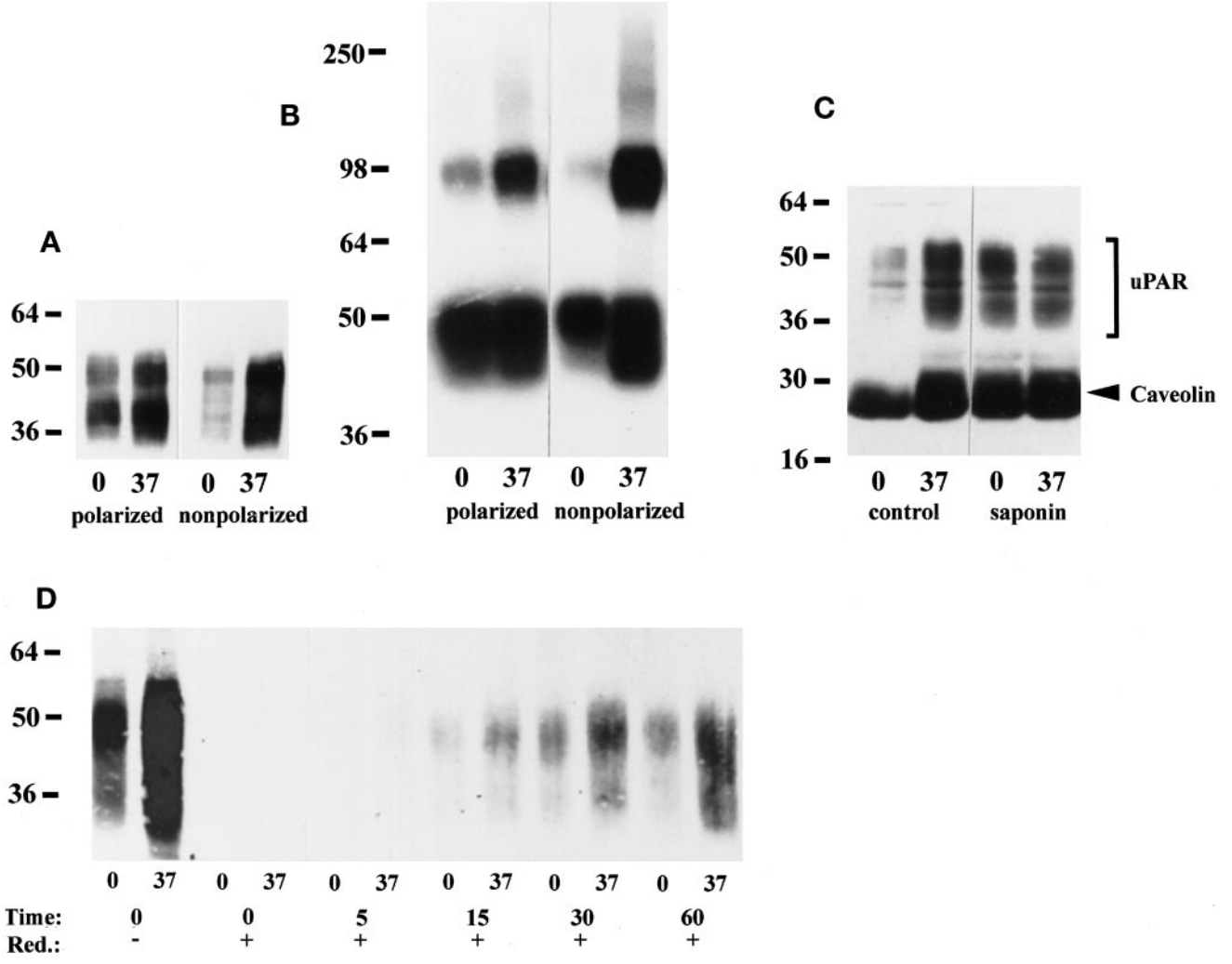

Figure 7. The fraction of detergent-soluble uPAR is lower in nonpolarized than polarized MDCK cells. (A) Polarized or nonpolarized MDCK cells were extracted with 1% TX-100 (pH 7.4) on ice or at 37°C as indicated. Equal volumes of extract were separated by 10% SDS-PAGE, immobilized on nitrocellulose membranes, and Western blotted with uPAR antibodies as described in the legend to Figure 1A. The blot shown is representative of five experiments. (B) Polarized or nonpolarized MDCK cells were preincubated with 1 nM DFP-uPA at 4°C before chemical cross-linking with 1 mM DSS. TX-100 extracts were then prepared as described above and resolved by 10% SDS-PAGE. Dried gels were autoradiographed for 48 h. Cross-linked uPAR migrating at ~95 kDa and free DFP-uPA present at the bottom of the gel are evident. (C) Polarized MDCK cells were extracted with 1% TX-100 (pH 6.5) on ice or at 37°C without (−) or with (+) 0.2% saponin, before 4–20% SDS-PAGE and transfer to nictrocellulose membranes, which were probed with a mixture of polyclonal antibodies to uPAR (bracket) and caveolin (arrowhead). (D) Nonpolarized MDCK cells were surface biotinylated with NHS-SS-biotin on ice and then chased at 37°C for the indicated times before reduction with a membrane-impermeable reducing agent on ice. Control dishes were kept on ice throughout and were reduced (t = 0, +) or not (t = 0, −). TX-100 extraction was performed as in A, and uPAR was immunoprecipitated with rabbit antibodies before SDS-PAGE and Western blotting with HRP-conjugated streptavidin.

lated to the ability of GPI-anchored proteins to associate with membrane microdomains rich in glycosphingolipids and cholesterol (Simons and Ikonen, 1997). These glycolipid domains are soluble in the detergent TX-100 at 37°C but insoluble at 0–4°C (Brown and Rose, 1992). When polarized and nonpolarized MDCK cells were extracted with 1% TX-100 on ice, a significantly higher fraction of the total amount of uPAR (corresponding to extraction at 37°C) was detergent soluble in polarized cells (Figure 7A). Densitometric analysis showed that on average 67 ± 10% versus 31 ± 4% (mean ± SD; n = 5) of uPAR was detergent soluble at 0°C in polarized and nonpolarized cells, respectively. This difference in partitioning was also evident when radiolabeled DFP-uPA was cross-linked to uPAR with the bifunctional reagent DSS. Cross-linked uPAR:DFP-uPA complexes migrated at the expected ~100 kDa (Figure 7B), and

identity was verified by Western blotting with anti-uPAR antibodies. Densitometry showed that 39 versus 14% (n = 2) of cross-linked uPAR was detergent soluble in polarized and nonpolarized cells, respectively. Although the absolute fractions of detergent-soluble uPAR were substantially lower than assessed by Western blotting, both experimental conditions yielded an ~2.5-fold higher solubility of uPAR in polarized cells. When extraction was performed at pH 6.5, the fraction of detergent-soluble uPAR decreased in both polarized and nonpolarized MDCK cells (shown for polarized cells in Figure 7C; compare with Figure 7A). Irrespective of pH, detergent insolubility of uPAR required cholesterol, because 0.2% saponin (Cerneus *et al*., 1993; Rijnboutt *et al*., 1996; Naslavsky *et al*., 1997) completely solubilized uPAR (Figure 7C). Also, caveolin was enriched in the detergent-resistant fraction and solubilized by saponin. It has been reported that only the detergent-soluble plasma membrane pool of the folate receptor or alkaline phosphatase is internalized (Cerneus *et al*., 1993; Rijnboutt *et al*., 1996). To address this question we used a surface-labeling protocol with a reduction-sensitive biotin analogue. Nonpolarized MDCK cells were surface biotinylated on ice and subsequently chased at 37°C before reduction of remaining cell surface biotin with a membrane-impermeable reducing agent. As shown in Figure 7D, the low degree of detergent solubility of cell surface-resident uPAR was retained also in intracellular locations.

Postendocytic Sorting of uPAR in Polarized and Nonpolarized MDCK Cells Is Different

Like other GPI-anchored proteins (van den Bosch *et al*., 1988; Keller *et al*., 1992), the majority of endocytosed uPAR recycles to the cell surface in nonepithelial cells after receptor–ligand dissociation (Nykjær *et al*., 1997). However, when nonpolarized MDCK cells were incubated overnight with 100 nM uPA:PAI-1, a marked accumulation of uPAR was evident in LAMP-1–positive lysosomes (Figure 8, D–F). This lysosomal localization, although much less pronounced, was evident after 2 h of chase. In contrast, cells incubated with DFP-uPA showed little lysosomal labeling for uPAR (Figure 8, A–C), similarly to control cells incubated without ligand. In polarized MDCK cells, confocal imaging demonstrated uPAR localization on the apical plasma membrane and in a subapical compartment morphologically compatible with the apical recycling compartment (Cardone *et al*., 1994; Zacchi *et al*., 1998). However, colocalization of uPAR and LAMP-1 was not observed to any appreciable degree (Figure 8, G–I). These findings were confirmed by cryoimmunogold labeling. In polarized MDCK cells challenged with uPA:PAI-1, ~85% of total uPAR labeling was localized on the apical cell surface (Figure 9, A and B). Intracellularly, labeling was mostly present in small apical endosomes, likely associated with the apical recycling compartment, and in some cell profiles this localization was pronounced (Figure 9B). To a lesser degree, labeling of multivesicular bodies (Figure 9A) also was evident, but very little labeling in dense-core lysosomes was noted (our unpublished results).

These results indicate that uPA:PAI-1 specifically promoted partial lysosomal targeting of uPAR in nonpolarized cells. To quantitate this phenomenon we used two independent cryolabeling protocols. In the first, nonpolarized MDCK cells endocytosed prebound DFP-uPA or uPA:PAI-1 for 150 min, which roughly corresponds to cell surface clearance of uPA:PAI-1 as assessed by radioligand (Figure 2) and immunofluorescence experiments. Distribution of uPAR on the cell surface, in endosomes, and in lysosomes was then quantitated by double labeling with uPAR and MPR or LAMP-1 antibodies, respectively (Table 2). In nonpolarized MDCK cells, surface labeling of uPAR was mainly on the dorsal cell surface and was evenly distributed with no indication of clustering (Figure 9C). In cells preincubated with either DFP-uPA or uPA:PAI-1, intracellular uPAR labeling was observed in multivesicular bodies, tubulovesicular elements (Figure 9E), and vacuoles that did not colabel for either MPR or LAMP-1, and in endosomes and lysosomes where colocalization with MPR and LAMP was evident (Figure 9, D–G). Most markedly, uPA:PAI-1 increased localization of uPAR in MPR and LAMP-1–containing compartments approximately twofold over DFP-uPA–treated cells (see Table 2).

In an alternative approach, nonpolarized MDCK cells were preloaded with 20-nm cationized gold and then chased for 3 h in the presence of saturating concentrations of DFP-uPA or uPA:PAI-1 in the incubation medium. Cryosections were subsequently single labeled with anti-uPAR antibodies, and the distribution in lysosomes, operationally defined by their abundant content of cationized gold particles and aggregates (van Deurs *et al*., 1995), endosomes, and cell surface was determined (summarized in Table 3). Again, an increase in uPAR labeling in a subset of late and terminal compartments was seen in uPA:PAI-1– relative to DFP-uPA–treated cells (Figure 9, H and I).

RAP Interferes with Intracellular Sorting of uPAR

When the fate of DFP-uPA or uPA:PAI-1 internalized during a 10-min pulse was examined, a three- to fourfold higher fraction of DFP-uPA could be recovered as free ligand in the medium or on the cell surface compared with uPA:PAI-1 (Figure 10), indicating recycling of uPAR-DFP-uPA. Conversely, degradation of uPA:PAI-1 was threefold higher than for DFP-uPA. Because uPA:PAI-1 seemingly directed sorting to lysosomes (Figures 8 and 9) but not endocytosis (Figures 2 and 3) of uPAR in nonpolarized cells, we speculated

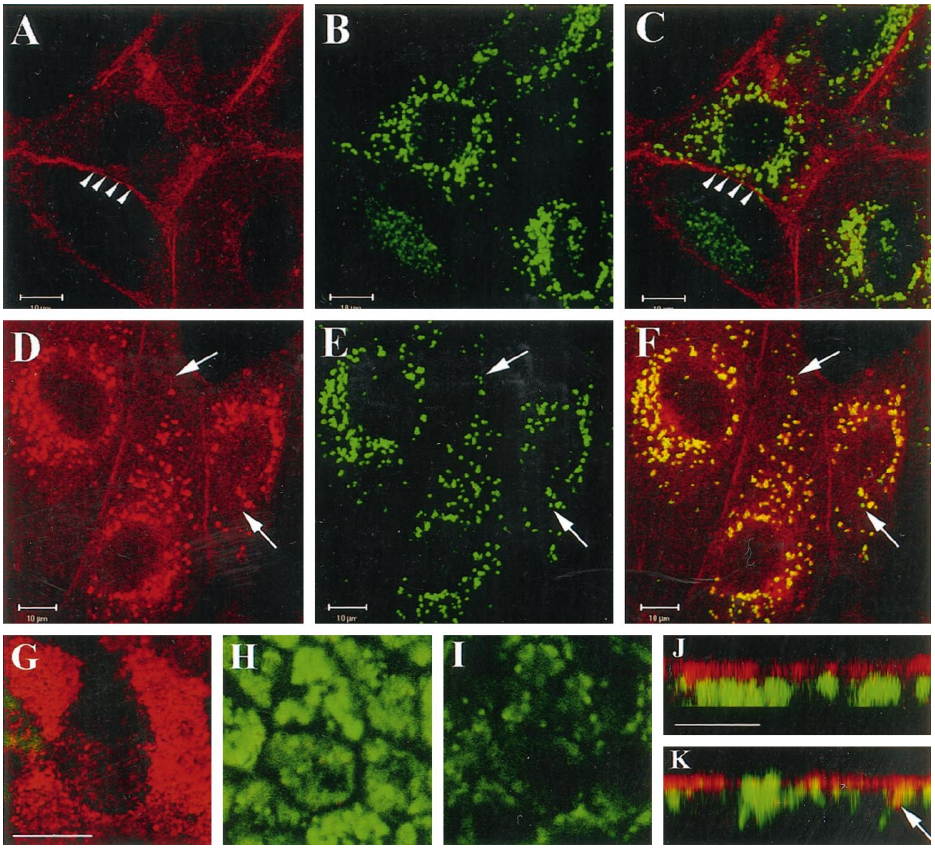

Figure 8. uPA:PAI-1 but not DFP-uPA causes accumulation of uPAR in lysosomes of nonpolarized MDCK cells. Nonpolarized (A–F) or filter-grown, polarized (G–K) MDCK cells were incubated with 100 nM DFP-uPA (A–C) or uPA:PAI-1 (D–K) in normal growth medium containing lysosomal protease inhibitors for 18 h with one intermittent change of incubation medium. Cells were processed for double-label immunofluorescence with anti-uPAR monoclonal antibody R2 and polyclonal anti-LAMP-1 antibodies, respectively, followed by Texas Red–conjugated goat anti-mouse or FITC-conjugated goat anti-rabbit antibodies as appropriate. Images were acquired by confocal microscopy. Shown are the seperate channels for uPAR labeling (A and D) and LAMP-1 labeling (B and E) and merged channels (C, F, and G–K). In nonpolarized cells, a single focal plane through the center of the cells shows that uPA:PAI-1 (D–F), but not DFP-uPA (A–C), caused uPAR to colocalize with LAMP-1 in perinuclear lysosomes. Arrowheads in A and C point to uPAR labeling of lateral membranes; arrows in F point to lysosomes not labeled for uPAR. (G–I) Merged channels of focal planes through apical (G), medial (H), and bottom (I) sections of the polarized monolayer. uPAR expression in monolayers was often heterogenous, as seen in G. uPAR is confined to the apical region (note typical microvillar labeling in G), well separated from LAMP-1–positive intracellular compartments. This is also evident in J and K, which show representative x–z confocal views compiled from stacks of 12 integration frames. Some areas display slight colocalization (K, arrow), but mostly uPAR and LAMP-1 were spatially separated. Bars, 10 μm.

that intracellular pools of RAP-binding internalization coreceptors might be involved in this sorting. RAP included in the incubation medium throughout the experiment caused the fraction of degraded uPA:PAI-1 to decrease, and the fraction recycled to increase in a dose-dependent manner (Figure 10B). This effect was apparent also in polarized MDCK cells (Figure 10A). Degradation of DFP-uPA was moderately decreased by RAP, but no effect on the fraction recycled was observed.

DISCUSSION

Clathrin-independent Internalization of uPAR

Our results demonstrate that uPAR can be internalized by different mechanisms, including clathrin-independent endocytosis. The most direct evidence is the continued internalization of uPA:PAI-1 in HeLa^{K44A} cells, in which clathrin-coated pit endocytosis is blocked after expression of the dynamin mutant. In the case of polarized MDCK cells this mechanism, corresponding to the low RAP noninhibitable internalization of uPAR ligands from the apical domain (Figure 2, A and C), is of minor importance in internalization of uPA:PAI-1 (Figure 2B), which is rapidly endocytosed through clathrin-coated pits, likely after association of uPAR-uPA:PAI-1 with internalization receptors of the LDLR family (Andreasen *et al.*, 1994; Conese *et al.*, 1995; Heegaard *et al.*, 1995). However, it could be selectively up-regulated by activators of adenylate cyclase and protein kinase C, which have been demonstrated to selectively up-regulate apical

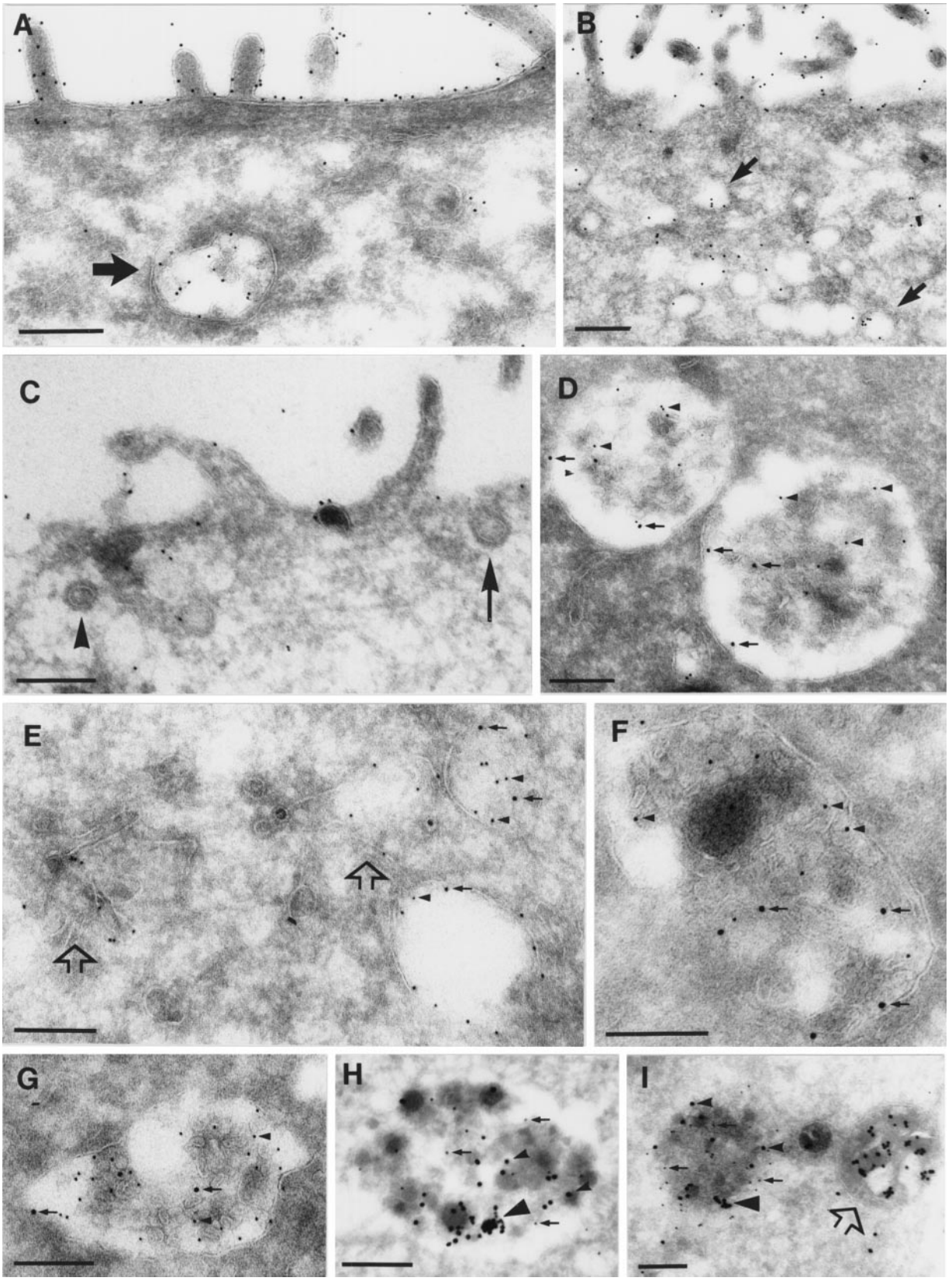

Figure 9.

Table 2. Cryoimmunogold quantitation of ligand-induced redistribution of uPAR

Ligand	Plasma-membrane (%)	Vesicles and vacuoles (%)[a]	Endosomes (%)[b]	Lysosomes (%)[c]	Total gold particle count	No. of cell profiles counted
DFP-uPA	78.0 ± 2.8	12.5 ± 0.7	9.0 ± 1.4		2376 (n=3)	21
	78.0 ± 2.0	16.3 ± 2.1		6.0 ± 0.0	2478 (n=2)	17
uPA/PAI	60.0 ± 15.1	28.8 ± 13.2	14.0 ± 4.0		3523 (n=3)	17
	56.3 ± 16.4	32.0 ± 13.2		11.3 ± 2.9	1580 (n=3)	20

Nonpolarized MDCK cells that had internalized prebound DFP-uPA or uPA:PAI-1 for 150 min were processed for cryoimmunogold double labeling using the antibody combinations uPAR/MPR or uPAR/LAMP-1, respectively. Antibodies were detected with 10 or 15 nm gold-conjugated protein A and quantitated. Means and SDs from two or three independent experiments are shown (multiple grids from each experiment were counted).

[a] Percentage of total uPAR gold particle count located in vesicles and vacuoles containing labeling exclusively for uPAR.

[b] Percentage of total number of uPAR gold particles colocalized with at least two MPR gold particles.

[c] Percentage of total number of uPAR gold particles colocalized with at least two LAMP-1 gold particles.

Table 3. Lysosomal accumulation of uPAR in nonpolarized MDCK cells preloaded with cationized 20-nm colloidal gold and chased in the presence of 100 nM DFPuPA or uPA:PAI-1 for 3 h

Ligand	Plasma membrane (%)	Compartments with <4 20-nm gold particles (%)	Compartments with at least 4 20 nm gold particles (%)	Total uPAR gold particle count	No. of cell profiles counted
DFP-uPA	74.8 ± 11.6	23.1 ± 9.8	1.1 ± 0.1	2286 (n=3)	21
uPA/PAI	58.6 ± 8.6	31.6 ± 6.7	9.85 ± 1.9	1339 (n=2)	16

Cryosections were single labeled with anti-uPAR antibodies followed by 10 nm gold-conjugated protein A, and distribution of labeling on plasma membrane or in endocytic compartments containing either less than four dispersed or more than four, mostly aggregated, 20-nm gold particles was determined.

clathrin-independent internalization in MDCK cells (Eker *et al*., 1994; Holm *et al*., 1995). In contrast, the RAP noninhibitable internalization in nonpolarized MDCK cells was approximately twofold higher, and even uPA:PAI-1 was preferentially endocytosed through this pathway. Internalization of uPAR was significantly higher in nonpolarized MDCK cells than reported for most GPI proteins (Lemansky *et al*., 1990; Lisanti *et al*., 1990; Keller *et al*., 1992; Cerneus *et al*., 1993) but comparable to endocytosis of 5′-nucleotidase (van den Bosch *et al*., 1988). Internalization of prebound [^{125}I]uPA:PAI-1 was not inhibited by an excess of unlabeled ligand, and together with the high internal steady-state fraction of DFP-uPA, the results indicate that uPAR to a large degree was endocytosed by a ligand-independent mechanism. Notably, uPA:PAI-1 endocytosis could not be accounted for by bulk membrane internalization, because it was higher than ricin uptake, indicating that endocytosis was facilitated. It is possible that MPR, which directly binds uPAR independently of uPA or uPA:PAI-1 occupancy (Nykjær *et al*., 1998), contributes to this uptake by mediating ligand-independent endocytosis of uPAR through

Figure 9 (facing page). uPA:PAI-1 causes partial redistribution of uPAR to late endosomes and lysosomes in nonpolarized MDCK cells. (A and B) Polarized MDCK cells; (C–I) nonpolarized MDCK cells. Cells internalized prebound uPA:PAI-1 for 150 min at 37°C (A–G) or, alternatively, were loaded with cationized 20-nm gold for 5 h, chased in DMEM-BSA alone for 3 h, and then incubated with 50 nM uPA:PAI-1 for 3 h in DMEM-BSA containing 10 μg/ml cycloheximide (G and H). Ultrathin cryosections were labeled with anti-uPAR antibodies followed by 10 nm gold-conjugated protein A (A–C, H, and I) or double labeled with secondary anti-MPR (D and E) or anti-LAMP (F and G) antibodies followed by 15 nm gold-conjugated protein A. (A and B) In polarized MDCK cells uPAR was mainly expressed on the cell surface but was also present in multivesicular bodies (A, large arrow) or in small apical endosomes (B, arrows). (C) Cell surface expression of uPAR in nonpolarized MDCK cells. The arrow points to a clathrin-coated pit; the arrowhead points to an apparent clathrin-coated vesicle. (D) Colocalization of uPAR (arrowheads) and MPR (arrows) in large endosomes with internal membrane structures. (E) uPAR (arrowheads) and MPR (arrows) colocalize in endosomes, but tubulovesicular structures (open arrows) show exclusive labeling for uPAR. (F and G) Colocalization of uPAR (arrowheads) and LAMP-1 (arrows) in dense lysosomal compartments. (H and I) uPAR (arrows) and cationized 20-nm gold particles (arrowheads) colocalize in compact lysosomes. Note the presence of aggregated, cationized gold particles (large arrowheads). (I) The open arrow points to a lysosome with many cationized-gold clusters but no uPAR. Bars, 250 nm.

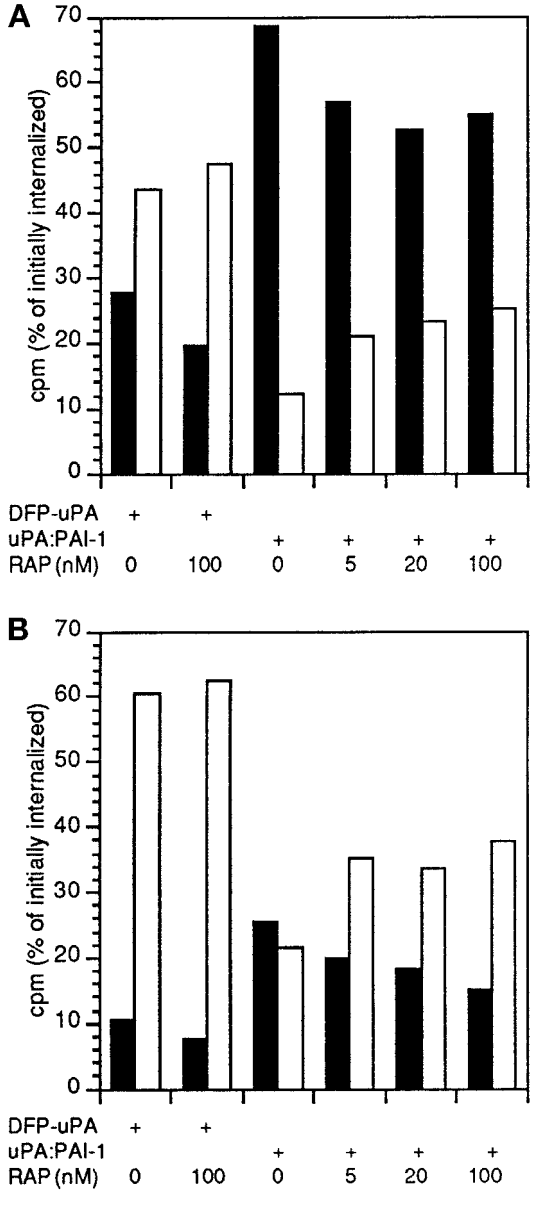

Figure 10. Fate of preinternalized DFP-uPA or uPA:PAI-1 in polarized or nonpolarized MDCK cells in the absence or presence of RAP. Polarized (A) or nonpolarized (B) cells were incubated with 500 pM [^{125}I]DFP-uPA or [^{125}I]uPA:PAI-1 for 90 min at 4°C in the absence or presence of the indicated concentrations of RAP. After washing on ice, cells were incubated at 37°C for 10 min to allow internalization of ligand. Surface-bound ligand was then removed by acid washing on ice, and cells returned to 37°C for a further 40 min with or without the indicated concentrations of RAP in the presence of 100 nM unlabeled uPA in the incubation medium to prevent reinternalization of recycled ligand. Degraded ligand represented by TCA-soluble counts per minute in the medium (black bars) or recycled ligand recovered on the cell surface or as TCA-insoluble counts in the medium (white bars) were expressed as percentage of counts internalized after the 10-min incubation. Means of two independent experiments in duplicate are shown. Variation was <10%.

clathrin-coated pits, but for reasons mentioned below we favor a predominant clathrin-independent mechanism of uPAR internalization also in nonpolarized cells.

Our data do not allow us to conclude whether the mechanisms responsible for the clathrin-independent endocytosis in nonpolarized cells or from the apical domain of polarized cells, respectively, are identical. However, several factors could contribute to a greater significance of a clathrin-independent internalization mechanism in nonpolarized cells. First, clathrin-independent endocytosis relative to clathrin-dependent endocytosis is more significant on the basolateral domain of MDCK cells (Eker *et al.*, 1994), which the plasma membrane of nonpolarized cells may share properties with. Second, signal-mediated concentration and internalization of transmembrane receptors and their ligands through clathrin-coated pits is decreased approximately 50% in low-density relative to high-density cell cultures (Hansen *et al.*, 1992), and a similar decrease in the internalization index of RAP was noted in nonpolarized MDCK cells. Third, the higher detergent insolubility of uPAR in nonpolarized cells could possibly reflect localization in glycolipid- and cholesterol-rich membrane microdomains, also termed rafts (Simons and Ikonen, 1997), which are known to include GPI-anchored proteins. Quantitation of the surface distribution of uPAR in nonpolarized cells showed that uPAR regardless of uPA:PAI-1 occupancy was largely excluded from clathrin-coated pits, as observed for other raft-associated proteins (Bretscher *et al.*, 1980; Roth *et al.*, 1986; Keller *et al.*, 1992; Scheiffele *et al.*, 1997). Only ~1% of uPAR labeling was present within coated pits, which themselves constituted 1.3% of the total surface area, giving a less than onefold concentration. For comparison the transferrin receptor is concentrated 5- to 10-fold in coated pits (Hansen *et al.*, 1992). Most likely, raft association restricts uPAR–uPA:PAI-1 interaction with internalization coreceptors, further diminishing the overall contribution of the clathrin-coated pit pathway in uPAR endocytosis. Alternatively, presence of uPAR in detergent-resistant membrane domains might, per se, predispose to selective internalization through a clathrin-independent pathway in nonpolarized MDCK cells. Interestingly, the internalized fraction of uPAR was mainly detergent insoluble. Our results are in contrast with reported data on alkaline phosphatase and folate receptor, which are almost completely detergent soluble in intracellular locations (Cerneus *et al.*, 1993; Rijnboutt *et al.*, 1996).

It has been proposed that caveolae are functionally and morphologically specialized rafts (Parton and Simons, 1995), which are able to mediate the selective internalization of some GPI-anchored proteins and glycolipids (Rothberg *et al.*, 1990; Keller *et al.*, 1992;

Parton, 1994; Parton *et al*., 1994). However, although uPAR in nonpolarized MDCK cells readily clustered in caveolae in the presence of cross-linking antibodies, as reported for other GPI-anchored proteins (Mayor *et al*., 1993; Parton *et al*., 1994), postfixation labeling showed only rare localization of uPAR in invaginated caveolae. In addition, clathrin-independent uptake in $HeLa^{K44A}$ cells or from the apical domain of MDCK cells was almost certainly not related to caveolae because of the very low level of caveolin and caveolae in $HeLa^{K44A}$ cells (our unpublished observations) and the basolateral expression of caveolae in polarized MDCK cells (Vogel *et al*., 1998).

Postendocytic Sorting of uPAR

In fibroblasts, uPAR has been shown to recycle to the cell surface (Nykjær *et al*., 1997), and slow recycling has also been established for other GPI proteins (van den Bosch *et al*., 1988; Keller *et al*., 1992; Shyng *et al*., 1993). In polarized MDCK cells, uPAR was recycled with high efficiency. Even after extended incubation periods in the presence of uPA:PAI-1, very little or no lysosomal accumulation of uPAR was revealed by morphological techniques. In contrast, by cryoimmunogold labeling protocols we estimate that 5–10% of internalized uPAR is sorted to lysosomes in nonpolarized MDCK cells per round of endocytosis, significantly decreasing the half-life of uPAR. It has been suggested that GPI-anchored proteins are recycled with slower kinetics than transmembrane receptors and bulk membrane because the GPI anchor confers cholesterol-dependent retention in early endosomes (Maxfield and Mayor, 1997). Also, sphingomyelin, which is enriched in detergent-insoluble glycolipid-rich membrane microdomains (Brown and Rose, 1992), is sorted to lysosomes in dedifferentiated HT29 epithelial cells but trafficks identically with transferrin receptor in differentiated clones (Kok *et al*., 1991). These results indicate that lipid sorting can occur in the endocytic pathway and, taken together with the detergent insolubility of endocytosed uPAR, suggest that lysosomal targeting of uPAR in nonpolarized MDCK cells could be a consequence of raft-mediated retention of uPAR in maturing endosomes.

Surprisingly, however, although uPAR internalization in nonpolarized cells was largely constitutive, lysosomal sorting of uPAR required uPA:PAI-1 and was partially interfered with by RAP, indicating that postendocytic sorting of uPAR was a ligand-regulated event. This is not compatible with a raft-based sorting mechanism, because sorting would be a function of lipid anchoring and would therefore be expected to cause lysosomal targeting of uPAR, irrespective of the nature of the ligand. Megalin and LRP are reycling receptors such as the LDLR itself, but at ultrastructural resolution both receptors have been identified in late endosomes and/or lysosomes (Bu *et al*., 1994; Christensen *et al*., 1995; Czekay *et al*., 1997). Interestingly, the endocytic itinerary of megalin is also regulated in a ligand-dependent manner (Czekay *et al*., 1997). Although megalin–lipoprotein lipase complexes dissociated in early endosomes, and megalin was recycled from this compartment, megalin-RAP travelled to late endosomes before dissociation and recycling of megalin. We therefore propose that uPA:PAI-1 may cause a similar trafficking of RAP-binding internalization receptors in nonpolarized MDCK cells and as a consequence mediate a translocation of uPAR to later endocytic compartments. Such a mechanism does not exclude incorporation of uPAR into detergent-resistant membrane domains in late endocytic compartments, perhaps assisted by the low pH in these compartments. It is known that the scrapie isoform of the GPI-anchored prion protein, which is localized mainly in late endosomes and lysosomes, is present in detergent-insoluble membrane domains (Vey *et al*., 1996), and recently it was shown that the internal membranes of late endosomes contain large amounts of a unique lipid that is involved in sorting of MPR to the TGN (Kobayashi *et al*., 1998).

ACKNOWLEDGMENTS

We thank Ulla Hjortenberg, Mette Ohlsen, Keld Ottesen, and Kirsten Pedersen for expert technical assistance and Fritz von Bülow for help with the confocal and electron microscopes. Anders Nykjær is greatly acknowledged for discussions and help in synthesis of uPA:PAI-1 complexes, Erik Ilsø Christensen for constructive criticism of the manuscript, and Ulla Vogel for help in plasmid construction and transfection. Pernille Vejbjerg is thanked for encouragement and helpful suggestions. This work was supported by the Danish Cancer Society, the Danish Medical Research Council, the Novo Nordisk Foundation, the Human Frontier Science Program (grant RG404/96 M) and a NATO Collaborative Research grant (CRG 900517) (to B.v.D. and K.S.).

REFERENCES

Andreasen, P.A., Sottrup-Jensen, L., Kjøller, L., Nykjær, A., Moestrup, S.K., Munch Petersen, C., and Gliemann, J. (1994). Receptor-mediated endocytosis of plasminogen activators and activator/inhibitor complexes. FEBS Lett. *338*, 239–245.

Bretscher, M.S., Thomson, N., and Pearse, B.M.F. (1980). Coated pits act as molecular filters. Proc. Natl. Acad. Sci. USA *77*, 4156–4159.

Brown, D.A., and Rose, J.K. (1992). Sorting of GPI-anchored proteins to glycolipid-enriched membrane subdomains during transport to the apical cell surface. Cell *68*, 533–544.

Bu, G., Geuze, H.J., Strous, G.J., and Schwartz, A.L. (1995). 39 kDa receptor-associated protein is an ER resident protein and molecular chaperone for LDL receptor-related protein. EMBO J. *14*, 2269–2280.

Bu, G., Maksymovitch, E.A., Geuze, H., and Schwartz, A.L. (1994). Subcellular localization and endocytotic function of low density lipoprotein receptor-related protein in human glioblastoma cells. J. Biol. Chem. *269*, 29874–29882.

Busso, N., Masur, S.K., Lazega, D., Waxman, S., and Ossowski, L. (1994). Induction of cell migration by pro-urokinase binding to its

receptor: possible mechanism for signal transduction in human epithelial cells. J. Cell Biol. *126*, 259–270.

Cardone, M.H., Smith, B.L., Song, W., Mochly-Rosen, D., and Mostov, K. (1994). Phorbol myristate acetate-mediated stimulation of transcytosis and apical recycling in MDCK cells. J. Cell Biol. *124*, 717–727.

Cerneus, D.P., Ueffing, E., Posthuma, G., Strous, G.J., and van der Ende, A. (1993). Detergent insolubility of alkaline phosphatase during biosynthetic transport and endocytosis. J. Biol. Chem. *268*, 3150–3155.

Chen, W.-J., Goldstein, J.L., and Brown, M.S. (1990). NPXY, a sequence often found in cytoplasmic tails, is required for coated pit-mediated internalization of the low density lipoprotein receptor. J. Biol. Chem. *265*, 3116–3123.

Christensen, E.I., Nielsen, S., Moestrup, S.K., Borre, C., Maunsbach, A.B., de Heer, E., Ronco, P., Hammond, T.G., and Verroust, P. (1995). Segmental distribution of the endoytosis receptor gp330 in renal proximal tubules. Eur. J. Biochem. *66*, 349–364.

Conese, M., and Blasi, F. (1995). Urokinase/Urokinase receptor system: Internalization/degradation of urokinase-serpin complexes: mechanism and regulation. Biol. Chem. Hoppe-Seyler *376*, 143–155.

Conese, M., Nykjær, A., Petersen, C.M., Cremona, O., Pardi, R., Andreasen, P.A., Gliemann, J., Christensen, E.I., and Blasi, F. (1995). α-2 macroglobulin receptor/LDL receptor-related protein (LRP)-dependent internalization of the urokinase receptor. J. Cell Biol. *131*, 1609–1622.

Conese, M., Olson, D., and Blasi, F. (1994). Protease Nexin-1-urokinase complexes are internalized and degraded through a mechanism that requires both urokinase receptor and α2-macroglobulin receptor. J. Biol. Chem. *269*, 17886–17892.

Cubellis, M.V., Wun, T.-C., and Blasi, F. (1990). Receptor-mediated internalization and degradation of urokinase is caused by its specific inhibitor PAI-1. EMBO J. *9*, 1079–1085.

Czekay, R.-P., Orlando, R.A., Woodward, L., Lundstrom, M., and Farquhar, M.G. (1997). Endocytotic trafficking of megalin/RAP complexes: dissociation of the complexes in late endosomes. Mol. Biol. Cell *8*, 517–532.

Damke, H., Baba, T., Warnock, D.E., and Schmid, S.L. (1994). Induction of mutant dynamin specifically blocks endocytic coated vesicle formation. J. Cell Biol. *127*, 915–934.

Danø, K., Behrendt, N., Brunner, N., Ellis, V., Ploug, M., and Pyke, C. (1994). The urokinase receptor: protein structure and role in plasminogen activation and cancer invasion. Fibrinolysis *8*(suppl 1), 189–203.

Eker, P., Kaae Holm, P., van Deurs, B., and Sandvig, K. (1994). Selective regulation of apical endocytosis in polarized Madin-Darby canine kidney cells by mastoparan and cAMP. J. Biol. Chem. *269*, 18607–18615.

Estreicher, A., Muhlhauser, J., Carpentier, J.-L., Orci, L., and Vassalli, J.-D. (1990). The receptor for urokinase type plasminogen activator polarizes expression of the protease to the leading edge of migrating monocytes and promotes degradation of enzyme inhibitor complexes. J. Cell Biol. *111*, 783–792.

Fazioli, F., Resnati, M., Sidenius, N., Higashimoto, Y., Appella, E., and Blasi, F. (1997). A urokinase-sensitive region of the human urokinase receptor is responsible for its chemotactic activity. EMBO J. *16*, 7279–7286.

Gorodinsky, A., and Harris, D.A. (1995). Glycolipid-anchored proteins in neuroblastoma cells form detergent-resistant complexes without caveolin. J. Cell Biol. *129*, 619–627.

Hannan, L.A., Lisanti, M.P., Rodriquez-Boulan, E., and Edidin, M. (1993). Correctly sorted molecules of a GPI-anchored protein are clustered and immobile when they arrive at the apical surface of MDCK cells. J. Cell Biol. *120*, 353–358.

Hansen, S.H., Sandvig, K., and van Deurs, B. (1992). Internalization efficiency of the transferrin receptor. Exp. Cell Res. *199*, 19–28.

Heegaard, C.W., Wiborg Simonsen, A.C., Oka, K., Kjøller, L., Christensen, A., Madsen, B., Ellgaard, L., Chan, L., and Andreasen, P.A. (1995). Very low density lipoprotein receptor binds and mediates endocytosis of urokinase-type plasminogen activator-type-1 plasminogen activator inhibitor complex. J. Biol. Chem. *270*, 20855–20861.

Herz, J., Clouthier, D.E., and Hammer, R.E. (1992). LDL receptor-related protein internalizes and degrades uPA-PAI-1 complexes and is essential for embryo implantation. Cell *71*, 411–421.

Holm, P.K., Eker, P., Sandvig, K., and van Deurs, B. (1995). Phorbol myristate selectively stimulates apical endocytosis via protein kinase C in polarized MDCK cells. Exp. Cell Res. *217*, 157–168.

Høyer-Hansen, G., Ploug, M., Behrendt, N., Rønne, E., and Danø, K. (1997). Cell-surface acceleration of urokinase-catalyzed receptor cleavage. Eur. J. Biochem. *243*, 21–26.

Johansen, T.E., Scholler, M.S., Tolstoy, S., and Schwartz, T.W. (1990). Biosynthesis of peptide precursors and protease inhibitors using new constitutive and inducible eukaryotic expression vectors. FEBS Lett. *267*, 289–294.

Keller, G.-A., Siegel, M.W., and Caras, I.W. (1992). Endocytosis of glycophospholipid-anchored and transmembrane forms of CD4 by different endocytotic pathways. EMBO J. *11*, 863–874.

Keller, P., and Simons, K. (1998). Cholesterol is required for surface transport of influenza virus hemagglutinin. J. Cell Biol. *140*, 1357–1367.

Kerjaschki, D., and Farquhar, M.G. (1983). Immunocytochemical localization of the Heymann nephritis antigen (gp330) in glomerular epithelial cells of normal Lewis rats. J. Exp. Med. *157*, 667–686.

Kjøller, L., Wiborg Simonsen, A.C., Ellgaard, L., and Andreasen, P.A. (1995). Differential regulation of urokinase-type-1 inhibitor complex endocytosis by phorbol esters in different cell lines is associated with differential regulation of a2-macroglobulin receptor and urokinase receptor expression. Mol. Cell. Endocrinol. *109*, 209–217.

Kobayashi, T., Stang, E., Fang, K.S., de Moerloose, P., Parton, R.G., and Gruenberg, J. (1998). A lipid associated with the antiphospholipid syndrome regulates endosome structure and function. Nature *392*, 193–197.

Kok, J.W., Babia, T., and Hoekstra, D. (1991). Sorting of sphingolipids in the endocytic pathway of HT29 cells. J. Cell Biol. *114*, 231–239.

Lemansky, P., Fatemi, S.H., Gorican, B., Meyale, S., Rossero, R., and Tartakoff, A.M. (1990). Dynamics and longevity of the glycolipid-anchored membrane protein, Thy-1. J. Cell Biol. *110*, 1525–1531.

Li, H., Kuo, A., Kochan, J., Strickland, D., Kariko, K., Barnathan, E.S., and Cines, D.B. (1994). Endocytosis of urokinase-plasminogen activator inhibitor type 1 complexes bound to a chimeric transmembrane urokinase receptor. J. Biol. Chem. *269*, 8153–8158.

Limongi, P., Resnati, M., Hernandez-Marrero, L., Cremona, O., Blasi, F., and Fazioli, F. (1995). Biosynthesis and apical localization of the urokinase receptor in polarized MDCK epithelial cells. FEBS Lett. *369*, 207–211.

Lisanti, M.P., Caras, I.W., Gilbert, T., Hanzel, D., and Rodriquez-Boulan, E. (1990). Vectorial apical delivery and slow endocytosis of glycolipid-anchored fusion protein in transfected MDCK cells. Proc. Natl. Acad. Sci. USA *87*, 7419–7423.

Lisanti, M.P., and Rodriquez-Boulan, E. (1990). Glycophospholipid membrane anchoring provides clues to the mechanism of protein sorting in polarized epithelial cells. Trends Biochem. Sci. *15*, 113–118.

Maxfield, F.R., and Mayor, S. (1997). Cell surface dynamics of GPI-anchored proteins. Adv. Exp. Med. Biol. *419*, 355–364.

Mayor, S., Presley, J.F., and Maxfield, F.R. (1993). Sorting of membrane components from endosomes and subsequent recycling to the cell surface occurs by a bulk flow process. J. Cell Biol. *121*, 1257–1269.

Mayor, S., Rothberg, K.G., and Maxfield, F.R. (1994). Sequestration of GPI-anchored proteins in caveolae triggered by cross-linking. Science *264*, 1948–1951.

Moestrup, S.K., Kaltoft, K., Munck Petersen, C., Pedersen, S., Gliemann, J., and Christensen, E.I. (1990). Immunocytochemical identification of the human a2-macroglobulin receptor in monocytes and fibroblasts: monoclonal antibodies define the receptor as a monocyte differentiation antigen. Exp. Cell Res. *190*, 195–203.

Moestrup, S.K., Nielsen, S., Andreasen, P., Jørgensen, K.E., Nykjær, A., Røigaard, H., Gliemann, J., and Christensen, E.I. (1993). Epithelial glycoprotein-330 mediates endocytosis of plasminogen-activator inhibitor type-1 complexes. J. Biol. Chem. *268*, 16564–16570.

Naslavsky, N., Stein, R., Yanai, A., Friedlander, G., and Taraboulos, A. (1997). Characterization of detergent-insoluble complexes containing the cellular prion protein and its scrapie isoform. J. Biol. Chem. *272*, 6324–6331.

Nykjær, A., *et al*. (1998). Mannose 6-phosphate/Insulin-like growth factor-II receptor targets the urokinase receptor to lysosomes via a novel binding interaction. J. Cell Biol. *141*, 815–828.

Nykjær, A., Conese, M., Christensen, E.I., Olson, D., Cremona, O., Gliemann, J., and Blasi, F. (1997). Recycling of the urokinase receptor upon internalization of the uPA:serpin complexes. EMBO J. *16*, 2610–2620.

Nykjær, A., Munck Petersen, C., Christensen, E.I., Davidsen, O., and Gliemann, J. (1990). Urokinase receptors in human monocytes. Biochim. Biophys. Acta *1052*, 399–407.

Nykjær, A., *et al*. (1992). Purified α2-macroglobulin receptor/LDL receptor-related protein binds urokinase plasminogen activator inhibitor type-1 complex. J. Biol. Chem. *267*, 14543–14546.

Olson, D., Pollanen, J., Høyer-Hansen, G., Rønne, E., Sakaguchi, K., Wun, T.-C., Appella, E., and Blasi, F. (1992). Internalization of the urokinase-plasminogen activator inhibitor type-1 complex is mediated by the urokinase-receptor. J. Biol. Chem. *267*, 9129–9133.

Parton, R.G. (1994). Ultrastructural localization of gangliosides; GM1 is concentrated in caveolae. J. Histochem. Cytochem. *42*, 155–166.

Parton, R.G., Joggerst, B., and Simons, K. (1994). Regulated internalization of caveolae. J. Cell Biol. *127*, 1199–1215.

Parton, R.G., and Simons, K. (1995). Digging into caveolae. Science *269*, 1398–1399.

Ploug, M., Rønne, E., Behrendt, N., Jensen, A.L., Blasi, F., and Danø, K. (1991). Cellular receptor for urokinase plasminogen activator. J. Biol. Chem. *266*, 1926–1933.

Prydz, K., Brandli, A., Bomsel, M., and Simons, K. (1990). Surface distribution of the mannose 6-phosphate receptors in epithelial Madin-Darby canine kidney cells. J. Cell Biol. *265*, 12629–12635.

Rijnboutt, S., Jansen, G., Posthuma, G., Hynes, J.B., and Schornagel, J.H. (1996). Endocytosis of GPI-linked membrane folate receptor-a. J. Cell Biol. *132*, 35–47.

Roldan, A.L., Cubellis, M.V., Masucci, M.T., Behrndt, N., Lund, L.R., Danø, K., Appella, E., and Blasi, F. (1990). Cloning and expression of the receptor for human urokinase plasminogen activator, a central molecule in cell surface, plasmin dependent proteolysis. EMBO J. *9*, 467–474.

Roth, M.G., Doyle, C., Sambrook, J., and Gething, M.J. (1986). Heterologous transmembrane and cytoplasmic domains direct functional chimeric influenza virus hemagglutinins into the endocytic pathway. J. Cell Biol. *102*, 1271–1283.

Rothberg, K.G., Ying, Y., Kolhouse, J.F., Kamen, B.A., and Anderson, R.G.W. (1990). The glycophospholipid-linked folate receptor internalizes folate without entering the clathrin-coated pit endocytic pathway. J. Cell Biol. *110*, 637–649.

Rønne, E., Behrendt, N., Ellis, V., Ploug, M., Danø, K., and Høyer-Hansen, G. (1991). Cell-induced potentiation of the plasminogen system is abolished by a monoclonal antibody that recognizes the NH2-terminal domain of the urokinase receptor. FEBS Lett. *288*, 233–236.

Sandvig, K., Olsnes, S., Petersen, O.W., and van Deurs, B. (1987). Acidification of the cytosol inhibits endocytosis from coated pits. J. Cell Biol. *105*, 769–689.

Sargiacomo, M., Sudol, M., Tang, Z., and Lisanti, M.P. (1993). Signal transducing molecules and glycosyl-phosphatidylinositol-linked proteins form a caveolin-rich insoluble complex in MDCK cells. J. Cell Biol. *122*, 789–807.

Scheiffele, P., Roth G.M., and Simons, K. (1997). Interaction of influenza virus haemagglutinin with sphingolipid-cholesterol membrane domains via its transmembrane domain. EMBO J. *16*, 5501–5508.

Schnitzer, J.E., McIntosh, D.P., Dvorak, A.M., Liu, J., and Oh, P. (1995). Separation of caveolae from associated microdomains of GPI-anchored proteins. Science *269*, 1435–1439.

Shyng, S.-L., Huber, M.T., and Harris, D.A. (1993). A prion protein cycles between the cell surface and an endocytic compartment in cultured neuroblastoma cells. J. Biol. Chem. *268*, 15922–15928.

Simons, K., and Ikonen, E. (1997). Functional rafts in cell membranes. Nature *387*, 569–572.

Slot, J.W., Geuze, H.J., Gigengack, S., Lienhard, G.E., and James, D.E. (1991). Immunolocalization of the insulin regulatable glucose transporter in brown adipose tissue of the rat. J. Cell Biol. *113*, 123–135.

Solberg, H., Rømer, J., Brunner, N., Holm, A., Sidenius, N., Danø, K., and Høyer-Hansen, G. (1994). A cleaved form of the receptor for urokinase-type plasminogen activator in invasive transplanted human and murine tumors. Int. J. Cancer *58*, 877–881.

Stahl, A., and Mueller, B.M. (1995). The urokinase-type plasminogen activator receptor, a GPI-linked protein, is localized in caveolae. J. Cell Biol. *129*, 335–344.

van den Bosch, R.A., du Maine, A.P.M., Geuze, H.J., van der Ende, A., and Strous, G.J. (1988). Recycling of 5′-nucleotidase in a rat hepatoma cell line. EMBO J. *7*, 3345–3351.

van Deurs, B., Holm, P.K., Kayser, L., and Sandvig, K. (1995). Delivery to lysosomes in the human carcinoma cell line Hep-2 involves an actin filament-facilitated fusion between mature and preexisting lysosomes. Eur. J. Cell Biol. *66*, 309–323.

Vey, M., Pilkuhn, S., Wille, H., Nixon, R., DeArmond, S.J., Smart, E.J., Anderson, R.G.W., Taraboulus, A., and Prusiner, S.B. (1996). Subcellular colocalization of the cellular and scrapie prion proteins- in caveolae-like membranous domains. Proc. Natl. Acad. Sci. USA *93*, 14945–14949.

Vogel, U., Sandvig, K., and van Deurs, K. (1998). Expression of caveolin-1 and polarized formation of invaginated caveoale in Caco-2 and MDCK II cells. J. Cell Sci. *111*, 825–832.

Wei, Y., Lukashev, M., Simon, D.I., Bodary, S.C., Rosenberg, S., Doyle, M.V., and Chapman, H.A. (1996). Regulation of integrin function by the urokinase receptor. Science *273*, 1551–1555.

Wei, Y., Waltz, D.A., Rao, N., Drummond, R.J., Rosenberg, S., and Chapman, H.A. (1994). Identification of the urokinase receptor as an adhesion receptor for vitronectin. J. Biol. Chem. *269*, 32380–32388.

Willnow, T.E., Rohlman, A., Horton, J., Otani, H., Braun, J.R., Hammer, R.E., and Herz, J. (1996). RAP, a specialized chaperone, prevents ligand-induced ER retention and degradation of LDL receptor related endocytic receptors. EMBO J. *15*, 2632–2639.

Zacchi, P., Stenmark, H., Parton, R.G., Orioli, D., Lim, F., Giner, A., Mellman, I., Zerial, M., and Murphy, C. (1998). Rab17 regulates membrane trafficking through apical recycling endosomes in polarized epithelial cells. J. Cell Biol. *140*, 1039–1053.